

Article

Biomimetic Ketone Reduction by Disulfide Radical Anion

Sebastian Barata-Vallejo ^{1,2}, Konrad Skotnicki ³, Carla Ferreri ¹, Bronislaw Marciniak ⁴,
Krzysztof Bobrowski ³ and Chryssostomos Chatgililoglu ^{1,4,*}

- ¹ Istituto per la Sintesi Organica e la Fotoreattività (ISOF), Consiglio Nazionale delle Ricerche (CNR), Via P. Gobetti 101, 40129 Bologna, Italy; sebastian.barata@isof.cnr.it (S.B.-V.); carla.ferreri@isof.cnr.it (C.F.)
- ² Departamento de Ciencias Químicas, Facultad de Farmacia y Bioquímica, Universidad de Buenos Aires, Junin 954, Buenos Aires CP 1113, Argentina
- ³ Institute of Nuclear Chemistry and Technology, Dorodna 16, 03-195 Warsaw, Poland; k.skotnicki@ichtj.waw.pl (K.S.); kris@ichtj.pl (K.B.)
- ⁴ Center for Advanced Technology, Adam Mickiewicz University, Uniwersytetu Poznańskiego 10, 61-614 Poznań, Poland; marcinia@amu.edu.pl
- * Correspondence: chrys@isof.cnr.it; Tel.: +390-5-1639-8309

Abstract: The conversion of ribonucleosides to 2'-deoxyribonucleosides is catalyzed by ribonucleoside reductase enzymes in nature. One of the key steps in this complex radical mechanism is the reduction of the 3'-ketodeoxynucleotide by a pair of cysteine residues, providing the electrons via a disulfide radical anion (RSSR^{•-}) in the active site of the enzyme. In the present study, the bioinspired conversion of ketones to corresponding alcohols was achieved by the intermediacy of disulfide radical anion of cysteine (CysSSCys)^{•-} in water. High concentration of cysteine and pH 10.6 are necessary for high-yielding reactions. The photoinitiated radical chain reaction includes the one-electron reduction of carbonyl moiety by disulfide radical anion, protonation of the resulting ketyl radical anion by water, and H-atom abstraction from CysSH. The (CysSSCys)^{•-} transient species generated by ionizing radiation in aqueous solutions allowed the measurement of kinetic data with ketones by pulse radiolysis. By measuring the rate of the decay of (CysSSCys)^{•-} at $\lambda_{\max} = 420$ nm at various concentrations of ketones, we found the rate constants of three cyclic ketones to be in the range of 10^4 – 10^5 M⁻¹s⁻¹ at ~22 °C.

Keywords: biomimetic chemistry; cysteine; ketone reduction; free radicals; pulse radiolysis; kinetics



Citation: Barata-Vallejo, S.; Skotnicki, K.; Ferreri, C.; Marciniak, B.; Bobrowski, K.; Chatgililoglu, C. Biomimetic Ketone Reduction by Disulfide Radical Anion. *Molecules* **2021**, *26*, 5429. <https://doi.org/10.3390/molecules26185429>

Academic Editors: Igor Alabugin and Elena G. Bagryanskaya

Received: 6 August 2021

Accepted: 1 September 2021

Published: 7 September 2021

Publisher's Note: MDPI stays neutral with regard to jurisdictional claims in published maps and institutional affiliations.



Copyright: © 2021 by the authors. Licensee MDPI, Basel, Switzerland. This article is an open access article distributed under the terms and conditions of the Creative Commons Attribution (CC BY) license (<https://creativecommons.org/licenses/by/4.0/>).

1. Introduction

The comprehension of free radical reactivity taking place in naturally occurring processes can be very important for chemistry in two main ways: (1) inspiring new synthetic methods based on the same mechanisms that nature uses to prepare biomolecules, and (2) designing biomimetic models to simulate the free radical damages and to provide molecular libraries for mechanistic and biomarker discovery. Two successful examples of these approaches from our group are the syntheses of 5',8-cyclopurine lesions [1–3] and mono-trans PUFA isomers [4–6]. Indeed, there are strict relationships between reactivity involving free radicals and processes taking place in nature [7]. Since biological reactivity occurs in an aqueous environment, free radical chemistry can become attractive for realizing eco-friendly and high-yielding methodologies.

The radical chemistry associated with thiols (RSH) and disulfides (RSSR) plays important roles in nature, particularly in enzymes and proteins. One example is the conversion of ribonucleosides to 2'-deoxyribonucleosides, the monomers required for the construction of DNA, catalyzed by radical enzymes called ribonucleoside reductases (RNRs). There are three forms of the enzyme (classes I, II, and III) that are active in different species, with the former being active in eukaryotes and microorganisms, using ribonucleotide diphosphates as substrates [8–10]. An intriguing step in class I is the transfer from the tyrosyl radical to the thiol moiety in the active site where the ribonucleotide substrate waits for the

conversion. Figure 1 summarizes the complex mechanism of this transformation, which initially involves a reversible 3'-hydrogen atom abstraction by the thiyl radical generated from the cysteine residues in the active site (1). There follows the elimination of water with translocation of the radical center to C2' and quenching of the newly formed C2' radical by another cysteine residue (2). This generates the disulfide radical anion (RSSR^{•-}) that reduces the 3'-ketodeoxynucleotide (2→3) [11,12]. To complete the cycle, the C3' radical abstracts the hydrogen from the initial cysteine residue (3→4). The restoration of the two cysteine residues occurs by the intervention of thioredoxin reductase (TRR) and NADPH [8].

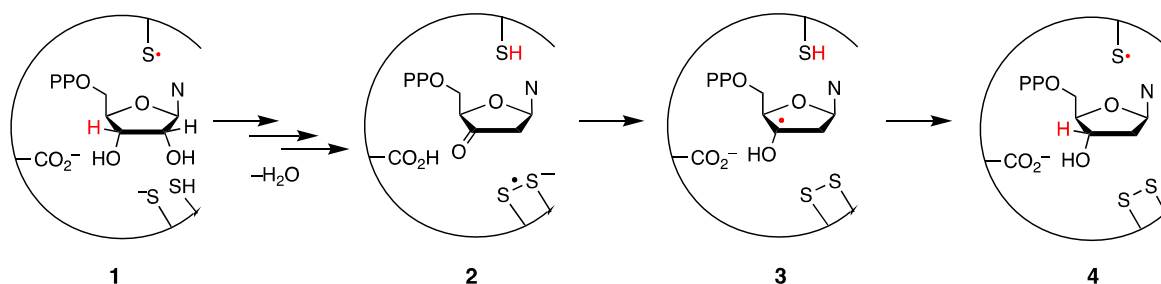
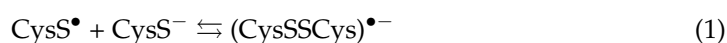


Figure 1. The transformation of ribonucleotides into 2'-ribose nucleotides by RNR.

We recently discovered that the sulfur radical species, derived at different pHs from hydrogen sulfide (H₂S), are able to transform 1,2-diols to alcohols via carbonyl reduction [13]. We hypothesized that the intermediate HSS^{•2-} is able to reduce the carbonyl moiety of ketones by a radical chain reaction. The HSS^{•2-} species is analogous to (CysSSCys)^{•-}, which may be able to reduce ketones to corresponding alcohols under certain conditions. It has been shown that disulfide radical anions (RSSR)^{•-} are strong reductants, with the standard reduction potential (*E*⁰) of the RSSR/RSSR^{•-} redox couple in the range 1.40–1.60 V vs. NHE [14–17]. The reduction potential *E*⁰ (RSSR/RSSR^{•-}) = −1.41 V found for the tripeptide glutathione disulfide is an indication of the reduction potential for the cysteine residue in proteins [18]. Disulfide radical anions in proteins are stabilized by the tertiary protein structures and do not readily dissociate to thiyl radical and thiolate anion (cf. Structure 2 in Figure 1).

Regarding cysteine (CysSH), which shows three p*K*_a values with the second one related to side chain thiol group (Figure 2A) [19], the equilibrium between (CysSSCys)^{•-} and thiolate and thiol, namely:



Is a complex reaction studied in some detail by different experimental methods [18,20,21]. The forward rate constant (*k*₁) was measured in the range pH 10–11 and found to be *k*₁ = 1.2 × 10⁹ M⁻¹s⁻¹, whereas the reverse rate constant (*k*₋₁) strongly depends on whether the amino group is protonated or not, affecting the disulfide radical anion equilibrium (Equation (1)) and the reduction potential of CysSSCys/CysSSCys^{•-} redox couple (Figure 2B). The stability of (CysSSCys)^{•-} increases when protonated amino groups are present and is reflected in equilibrium constants *K*₁: 438 M⁻¹ (with zero protonated amino groups) (5), 317 M⁻¹ (with one protonated amino group) (6), and 8900 M⁻¹ (with two protonated amino groups) (7). Increases in stability of these species are indicated by progressively less negative reduction potentials: −1.50 V, −1.38 V, and −1.30 V, for 0, 1, and 2 protonated amino groups, respectively [18].

Here, we report the photochemical conditions found to transform ketones to corresponding alcohols by CysSH via a radical chain reaction involving (CysSSCys)^{•-} as reducing species. We also discovered that the reduction of two selected substrates proceeds via a dual radical chain mechanism. Furthermore, we applied time-resolved spectroscopy (pulse

radiolysis) to generate $(\text{CysSSCys})^{\bullet-}$ by reaction of CysS^- with HO^\bullet radicals and provided the rate constants of both $(\text{CysSSCys})^{\bullet-}$ and HO^\bullet species with three cyclic ketones.

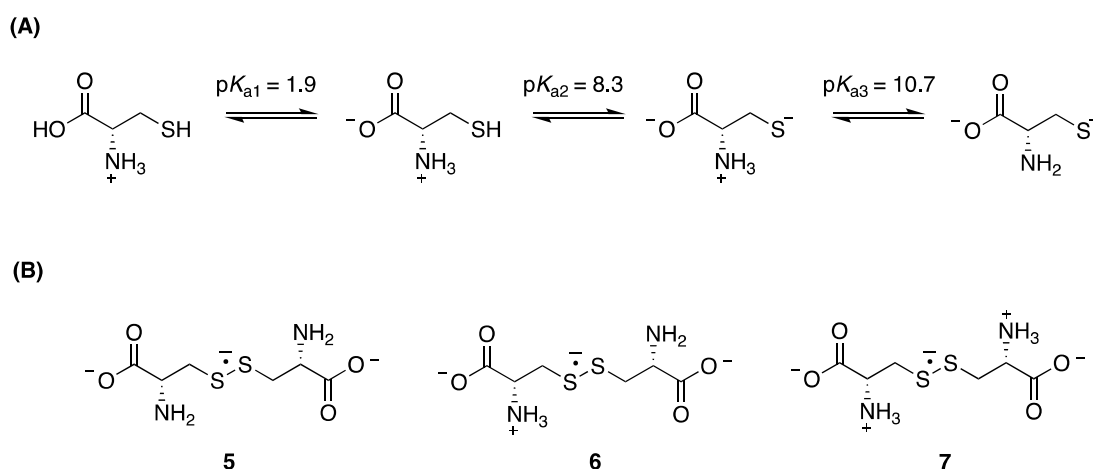


Figure 2. (A) The structure of cysteine, CysSH , and associated pK_a values; (B) Disulfide radical anion of cysteine $(\text{CysSSCys})^{\bullet-}$ with 0 (5), 1 (6), and 2 (7) protonated amino groups.

2. Results and Discussion

2.1. Ketone Reduction by the Photolysis of Cysteine-Containing Aqueous Solutions

2.1.1. Cyclohexanone Reduction and Optimization Studies at Different pH Values

The photolysis (low-pressure Hg lamp, 5.5 W) of N_2 -saturated aqueous solutions of cyclohexanone (**8**, 8.3 mM) containing CysSH (18.3 mM) was monitored for up to 60 min and at various pH values (7.0, 7.5, 8.5, 9.6, 10.6, 11.5, 12.0, and 13.0) adjusted with 5% NaOH. In all experiments, cyclohexanol (**9**) was the only product. Table 1 reports the conversion of **8** to **9** at 30 and 60 min at each pH value. As shown in Table 1, cyclohexanol formation is achieved successfully at all pH values studied, reaching a maximum product yield of 96% at pH 10.6.

Table 1. Photolysis (low-pressure Hg lamp, 5.5 W) of N_2 -saturated aqueous solutions of cyclohexanone (**8**, 8.3 mM) containing cysteine (18.3 mM) with formation of cyclohexanol (**9**) at different irradiation times and pH. ¹

pH (Initial)	Time (min)			pH (Final)
		8 (mM)	9 (mM)	
7.0	30	6.6	1.7	-
	60	5.1	3.2	6.0
7.5	30	5.5	2.8	-
	60	4.4	3.9	6.5
8.5	30	1.8	6.5	-
	60	1.0	7.3	7.5
9.6	30	1.9	6.4	-
	60	0.9	7.4	8.3
10.6	30	1.2	7.1	-
	60	0.3	8.0	9.5
11.5	30	1.7	6.6	-
	60	0.5	7.8	10.8
12.0	30	1.6	6.7	-
	60	0.6	7.7	11.5

¹ Reaction temperature was constant at 42 ± 1 °C.

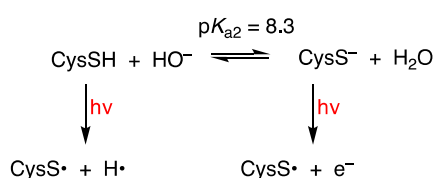
It is worth mentioning that other thiol derivatives such as 2-mercaptoethanol or *N*-acetylcysteine afford similar reductions but in lower yields (e.g., 51% and 56% after 60 min at pH 12, respectively) under identical experimental conditions.

2.1.2. Reaction Mechanism: Initiation Steps for a Radical Chain Process

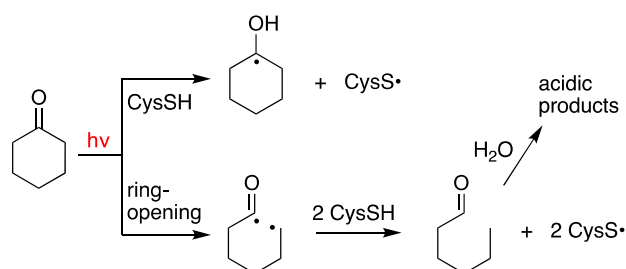
Based on the concentration of cyclohexanone and cysteine as well as their molar absorption coefficients, the light of 253.7 nm is absorbed by approximately 50% by each substrate. Light absorbed by the thiol/thiolate affords the thiyl radical together with H^\bullet/e^- (Figure 3a) [22]. Light absorbed by the cyclohexanone affords the S_1 (n,π^*) or T_1 (n,π^*) excited states. The T_1 state can react with thiol [23], whereas both S_1 and T_1 states are reported to lead to a classical type I cleavage (ring-opening) [24,25], and we suggest that this biradical intermediate can react with thiol (Figure 3a).

At pH 10.6, where the yield of ketone reduction is higher (cf. Table 1), the $CysS^-$ form is above 99%, being the pK_a value of SH moiety 8.3, although the concentration of CysSH is still $\sim 150 \mu M$. It is known that $CysS^\bullet$ adds reversibly to the parent anion to form the dimeric radical anion species, the forward reaction being close to the diffusion control rate (cf. Introduction). Therefore, due to the relatively high concentration of cysteine (18.3 mM), at higher pHs the main reactive species is $(CysSSCys)^\bullet$. We propose that **8** is reduced to ketyl radical anion **10** by the $RSSR^\bullet$, via single-electron transfer (SET). Subsequent protonation **10** \rightarrow **11** from the aqueous medium and H-atom abstraction from CysSH affords the product **9**, completing the radical chain mechanism (Figure 3b). The low concentration of CysSH ($\sim 150 \mu M$) is compensated by fast H-atom abstraction ($k_H > 10^8 M^{-1} s^{-1}$ for analogous reactions [26,27]). It is worth mentioning that the pK_a values associated with the hydroxyl protons of ketyl radical **11** and alcohol **9** are ~ 12.5 and 16, respectively [28,29]. The overall process is perhaps facilitated by a concerted proton-coupled electron transfer (PCET) affording the ketyl radical **11** from **8** [30].

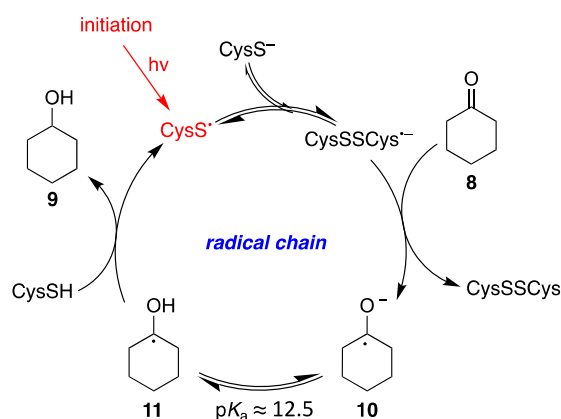
Photolysis of cysteine at 253.7 nm



Photolysis of cyclohexanone at 253.7 nm



(a)

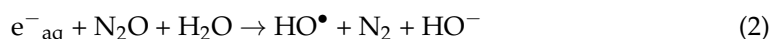


(b)

Figure 3. Proposed reaction mechanism for the reduction of cyclohexanone to cyclohexanol: (a) Possible initiation steps; (b) The radical chain reaction.

Next, we considered the reduction of **8** at pH 10.6 by changing the degassing conditions, i.e., N_2O - instead of N_2 -saturated solutions. It is well-known that N_2O -saturated

solutions (~ 0.02 M of N_2O) and e^-_{aq} are efficiently transformed into HO^\bullet radicals via Reaction 2 ($k = 9.1 \times 10^9 \text{ M}^{-1}\text{s}^{-1}$) [31].



In N_2O -saturated conditions, the yields of cyclohexanol are 22% and 26% after 30 and 60 min of irradiation, respectively, in comparison to 86% and 96% of cyclohexanol after 30 and 60 min under N_2 -saturated conditions. This suggests that the presence of N_2O strongly inhibits the radical chain reaction. Since $(\text{CysSSCys})^{\bullet-}$ does not react with N_2O , we suggest that the e^- generated by photolysis of CysS^- (cf. Figure 3a) undergo very fast hydration into hydrated electrons (e^-_{aq}) and then are trapped by N_2O . This finding indicates that the addition of e^-_{aq} to the carbonyl moiety of ketones is also an initiation step in the radical chain reaction described above.

Another important experimental observation is the decrease in pH during the reaction time (compare Columns 1 and 5 in Table 1). Tentatively, we suggest that after the ring-opening of the ketone triplet state and the reaction of biradical with thiol, the resulting aldehyde is the precursor of acidic products such as hydrated aldehyde. We could not obtain analytical evidences of by-products, probably due to their presence being below the detection limits.

2.1.3. Other Substrates for Ketone Reduction at pH 10.6

Considering the efficiency of the cyclohexanone reduction, the reduction of a few other ketones to the corresponding alcohols mediated by cysteine was further explored. Thus, under the optimized reaction conditions reported in Table 1 and at pH 10.6, ketones 12–15 all produced exclusively the corresponding alcohols, with yield $\geq 90\%$ (Figure 4).

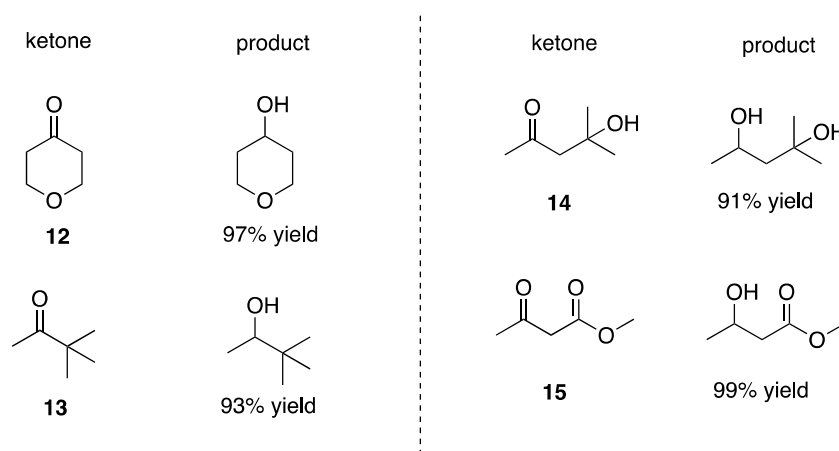


Figure 4. Reduction of ketones 12–15 to the corresponding alcohols. N_2 -saturated aqueous solutions of carbonyl compound (8.3 mM) cysteine (18.3 mM), pH adjusted to 10.6 at 42 ± 1 °C, were irradiated for 60 min. Yields by GC analysis based on products formation.

We demonstrated for the first time that the generation of ketyl radical anion via disulfide radical anion can be achieved. It is worth mentioning that: (i) SET reduction of ketones is a classical approach for the formation of ketyl radical anions, and such an approach has been used extensively in organic synthesis, as documented by the recently published tutorial review [32]; and (ii) ketyl radical anions formation have been typically carried out by means of dissolving metals such as Li, Na, and K, usually in liquid ammonia solution and in the presence of a proton source [33]. It can be envisaged that our bioinspired work will foster applications for SET methodology in aqueous environment.

2.1.4. The Reduction of 2-Hydroxycyclohexanone and 2-Cyclopenten-1-one at pH 10.6

For a better understanding of the reaction mechanism, we also considered the carbonyl reduction in 2-hydroxycyclohexanone (**16**) and 2-cyclopenten-1-one (**19**), having α -HO and internal α,β -unsaturated moiety, respectively.

Photolysis (low-pressure Hg lamp, 5.5 W) of N_2 -saturated aqueous solutions of 2-hydroxycyclohexanone **16** (8.3 mM) containing CysSH (18.3 mM) was carried out for different times (up to 60 min) at pH 10.6. Cyclohexanone (**8**) and cyclohexanol (**9**) were formed as the only products. Figure 5a displays a graph with the disappearance of **16** (\blacklozenge) and the formation of **8** (\bullet) and **9** (\blacktriangle) as a function of the reaction time, showing clearly that the reaction $16 \rightarrow 9$ occurs stepwise. The loss of **16** quantitatively matched the formation of **8** and **9**, with 17% and 82% yields, respectively, after 60 min. The mechanism is depicted in Figure 5b based on a dual radical chain process, starting from the reaction of $(\text{CysSSCys})^{\bullet-}$ with **16** to produce the ketyl radical anion **17**. This species undergoes α,β -C–O scission and HO^- elimination, with the shift of the radical center to produce **18** [27], which completes the catalytic cycle by reacting with CysSH regenerating CysS^\bullet . The so-formed cyclohexanone (**8**) undergoes a second radical chain reaction, as described in Figure 3b.

The reduction of 2-cyclopenten-1-one (**19**) was also explored under identical experimental conditions. The time profile of the reduction of (**19**) at pH 10.6 is reported in Figure 6a. In all experiments, cyclopentanone (**22**) and cyclopentanol (**23**) were formed as the only products, and again, the disappearance of **19** (\blacklozenge) and the formation of **22** (\bullet) and **23** (\blacktriangle) as a function of the reaction time showed clearly that the reaction $19 \rightarrow 23$ occurs stepwise. The loss of **19** quantitatively matched with the formation of **22** and **23**, with 23% and 77% yields, respectively, after 60 min. The mechanism depicted in Figure 6b is based again on a dual radical chain process, starting from the single-electron transfer from $(\text{CysSSCys})^{\bullet-}$ to **19** give the allyl-type radical **20**. This species undergoes protonation from the aqueous medium with double-bond shift to produce **21**, which completes the first catalytic cycle by reacting with CysSH regenerating CysS^\bullet . The so-formed cyclopentanone (**22**) undergoes a second radical chain reaction analogous to the one reported for cyclohexanone in Figure 3b.

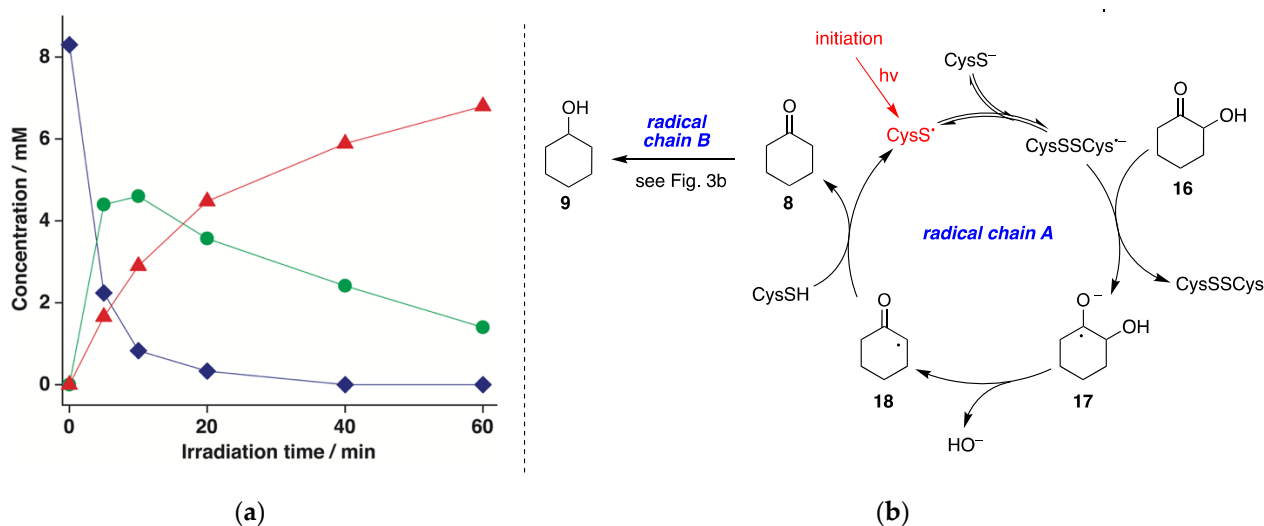


Figure 5. (a) Concentration of **16** (\blacklozenge), **8** (\bullet), and **9** (\blacktriangle) vs. irradiation time for the photolysis of N_2 -saturated 2-hydroxycyclohexanone (**16**) aqueous solutions (8.3 mM) containing CysSH (18.3 mM), pH adjusted to 10.6, at 42 ± 1 °C; (b) Proposed reaction mechanism involving dual radical chain reactions A and B.

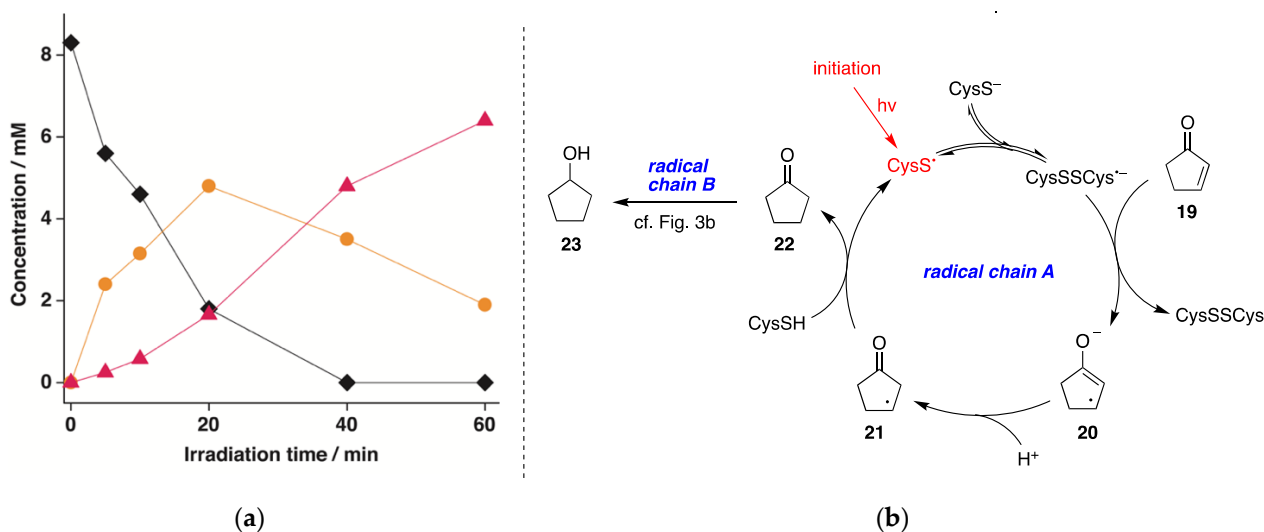
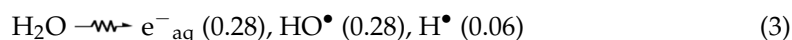


Figure 6. (a) Concentration of **19** (◆), **22** (●), and **23** (▲) vs. irradiation time for the photolysis of N_2 -saturated 2-cyclopenten-1-one (**19**) aqueous solutions (8.3 mM) containing CysSH (18.3 mM), pH adjusted to 10.6, at 42 ± 1 °C; (b) Proposed reaction mechanism involving dual radical chain reactions A and B.

2.2. Pulse Radiolysis Studies and Rate Constants of SET

Pulse irradiation of water leads to the primary reactive species e^-_{aq} , HO^\bullet , and H^\bullet , as shown in Reaction 3. The values in brackets represent the radiation chemical yield (G) in $\mu\text{mol J}^{-1}$. In N_2O -saturated solution (~ 0.02 M of N_2O), e^-_{aq} are efficiently transformed into HO^\bullet radicals via Reaction 1 ($k = 9.1 \times 10^9 \text{ M}^{-1}\text{s}^{-1}$), affording $G(HO^\bullet) = 0.56 \mu\text{mol J}^{-1}$ [34].



The reaction of HO^\bullet radicals with cysteine (100 mM) in the absence or in the presence of a ketone (up to 30 mM) was investigated in N_2O -saturated solutions at pH 10.6. These experimental conditions were chosen in order (i) to maximize the formation of thiyl radicals (Reaction 4, $k_4 = (5.35 \pm 0.82) \times 10^9 \text{ M}^{-1}\text{s}^{-1}$) [35], (ii) to minimize the quenching of HO^\bullet by ketones (Reaction 5, unknown rate constants), (iii) to convert the thiol moiety of cysteine into thiolate ions, (iv) to maximize conversion of thiyl radicals into $(CysSSCys)^\bullet-$ (Reaction 1), and (v) to facilitate the electron transfer between $(CysSSCys)^\bullet-$ and ketones (Reaction 6). Furthermore, at pH 10.6, two forms of disulfide radical anion **5** and **6** are present at similar concentrations (Figure 2B).



Transient absorption spectrum of $(CysSSCys)^\bullet-$ in the range 280–620 nm recorded 10 μs after the electron pulses is shown in Figure 7A, with the absorption maximum at 420 nm and in accord with previous reported ones [35]. The black traces in Figure 7B represent the decay of transient absorption at $\lambda_{\text{max}} = 420$ nm recorded after the electron pulse. The rate of decay of $(CysSSCys)^\bullet-$ was investigated by varying the concentrations of a ketone from 0 to 30 mM. We selected three ketones: cyclohexanone (**8**), 2-hydroxycyclohexanone (**16**), and cyclopentenone (**19**) for the time-resolved studies. The decay kinetics at various concentrations of **8**, **16**, and **19** were recorded at λ_{max} , as shown in Figure 7B, for the presence of 30 mM of **8** (blue), **16** (green) and **19** (red). The pseudo-first-order rate constants of the decay of 420 nm absorption band were plotted as a function of ketone concentration (Figure 7C).

It is clearly seen that the pseudo-first-order rate constants measured at $\lambda = 420$ nm show a linear dependence on the concentration of **8**, **16**, and **19** in the full range of concentration studied (Figure 7C). The slopes in Figure 7C represent the second-order rate constants for the decay of $(\text{CysSSCys})^{\bullet-}$ resulting from the reaction of $(\text{CysSSCys})^{\bullet-}$ with **8**, **16**, and **19** (Reaction 6). The obtained values of k_6 for three ketones are collected in Table 2. Both **16** and **19**, having α -HO and internal α,β -unsaturated moieties, increased the rate constant by 3.7- and 5.9-folds, respectively, due to extra stabilization of ketone radical anion.

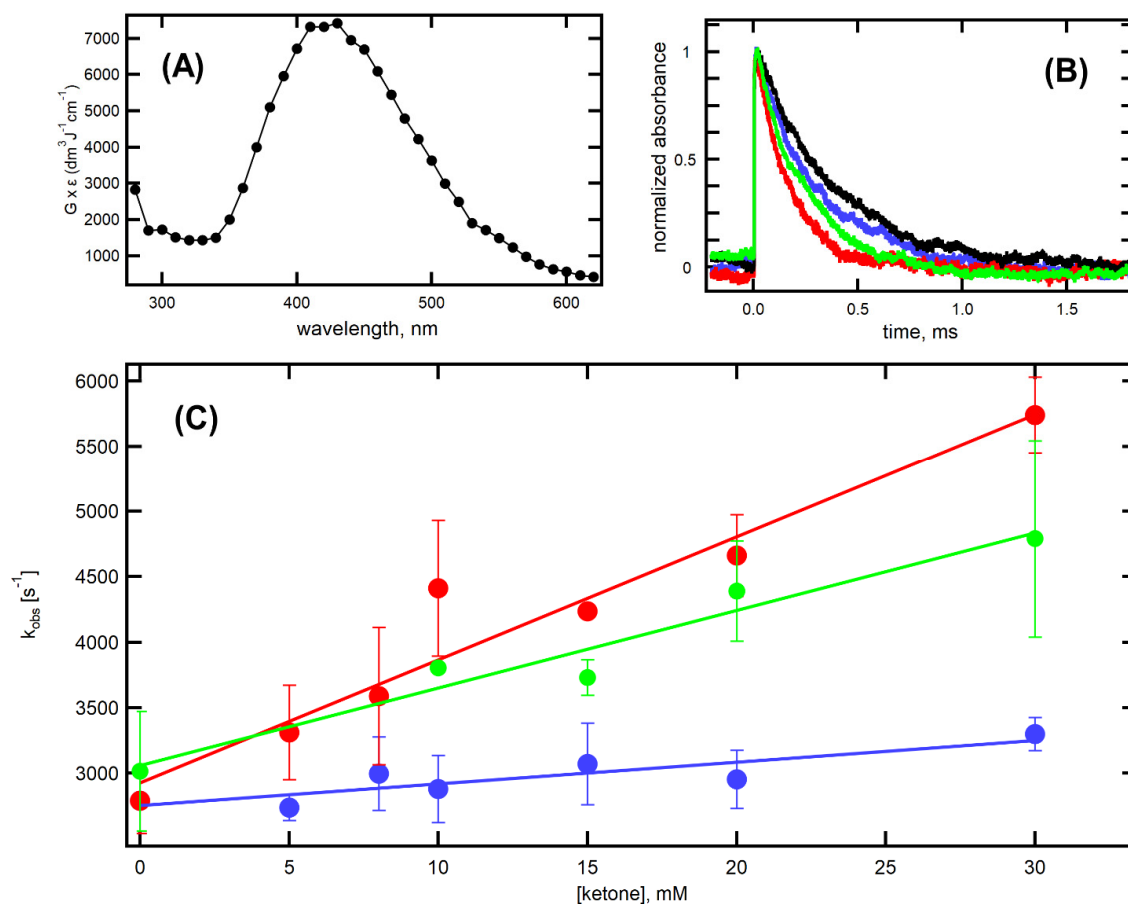
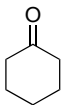
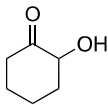
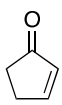


Figure 7. (A) Absorption spectrum of $(\text{CysSSCys})^{\bullet-}$ recorded 10 μs after the electron pulse in N_2O -saturated aqueous solutions at pH = 10.6 containing 100 mM of cysteine. (B) Normalized time profiles representing decay of transient absorption at $\lambda = 420$ nm, recorded after the electron pulse in N_2O -saturated aqueous solutions at pH = 10.6, containing 100 mM of cysteine in the absence of ketones (black) and in the presence of 30 mM of **8** (blue), **16** (green) and **19** (red). (C) Plots of the observed pseudo-first-order rate constants of the decay of the 420 nm absorption as a function of **8** (●), **16** (●) and **19** (●) concentration in N_2O -saturated aqueous solutions at pH = 10.6, containing 100 mM of cysteine.

Table 2. Rate constants ($\text{M}^{-1}\text{s}^{-1}$) for the reactions of $(\text{CysSSCys})^{\bullet-}$ and HO^{\bullet} with the three cyclic ketones. $(\text{CysSSCys})^{\bullet-}$ reacts by one-electron transfer and HO^{\bullet} reacts by H-atom abstraction. ¹.

k ($\text{M}^{-1}\text{s}^{-1}$)/Radical			
	8	16	19
$k_6/(\text{CysSSCys})^{\bullet-}$	$(1.6 \pm 0.3) \times 10^4$	$(5.9 \pm 0.5) \times 10^4$	$(9.4 \pm 0.2) \times 10^4$
k_5/HO^{\bullet}	7.2×10^7	8.6×10^7	1.3×10^8

¹ At room temperature (~ 22 °C).

By applying the common competition kinetics method [36], the rate constants for the reaction of HO• radicals with ketones (Reaction 5) can also be estimated. To our best knowledge, these rate constants were not measured earlier. Indeed, from the plot of the reciprocal of [CysSSCys^{•−}] versus the [CysSH]/[Ketone] ratio and considering $k_4 = (5.35 \pm 0.82) \times 10^9 \text{ M}^{-1}\text{s}^{-1}$, we obtained the values of k_5 reported in Table 2.

3. Materials and Methods

3.1. Materials and Instrumentation

All commercial chemicals were used as received unless otherwise noted. L-cysteine $\geq 98.5\%$, cyclohexanone $\geq 99.5\%$, cyclohexanol 99%, tetrahydro-4H-pyran-4-one 99%, tetrahydro-4-pyranol 98%, 3,3-dimethyl-2-butanone 97%, 3,3-dimethyl-2-butanol 98%, 4-hydroxy-4-methyl-2-pentanone 99%, hexylene glycol 99%, methyl acetoacetate 99%, methyl 3-hydroxybutyrate $\geq 95\%$, 2-hydroxycyclohexanone 99%, 2-cyclopenten-1-one 98%, cyclopentanone 99%, cyclopentanol 99%, 2-mercaptoethanol $\geq 99\%$, N-acetyl-L-cysteine European Pharmacopoeia Reference Standard, and phosphoric acid 85 wt% in water were obtained from Sigma-Aldrich (San Louis, MO, USA). Diethyl ether (HPLC grade) was obtained from Carlo Erba (Milan, Italy) and distilled before use. Water was purified with a Millipore system. Absorption spectra were recorded with a PerkinElmer Lambda 950 spectrophotometer (PerkinElmer, Shelton, USA). UV irradiations were performed in a micro-photochemical reaction assembly with quartz well (Ace Glass) using a 5.5 W cold cathode, low-pressure, mercury arc, and gaseous discharge lamp (corresponds to $\lambda = 250\text{--}260 \text{ nm}$) made of double-bore quartz (Ace Glass). Ethyl ether extracts of the irradiated samples were analyzed by GC-MS (Thermo Scientific Trace 1300, Waltham, MA, USA) equipped with a $15\text{ m} \times 0.25\text{ mm} \times 0.25\text{ }\mu\text{m}$ TG-SQC 5% phenyl methyl polysiloxane column, with helium as carrier gas, coupled to a mass selective detector (Thermo Scientific ISQ, Waltham, MA, USA).

3.2. Ketone Reduction

General procedure for the irradiation experiments. L-cysteine (13.3 mg, 0.11 mmol) was dissolved in 5 mL of N₂-saturated water while continuously bubbling N₂ in the photolysis apparatus. Cyclohexanone (4.9 mg, 0.05 mmol), tetrahydro-4H-pyran-4-one (5.0 mg, 0.05 mmol), 3,3-dimethyl-2-butanone (5.0 mg, 0.05 mmol), 4-hydroxy-4-methyl-2-pentanone (5.8 mg, 0.05 mmol), methyl acetoacetate (5.8 mg, 0.05 mmol), 2-hydroxycyclohexanone (5.7 mg, 0.05 mmol), or 2-cyclopenten-1-one (4.1 mg, 0.05 mmol) were added to the photolysis apparatus. The pH was adjusted to the specific value using a NaOH 5% *m/v* or a H₃PO₄ 5% *v/v* solution in deoxygenated water, and the final volume of the reaction was adjusted with N₂-saturated water in order to reach 6 mL. The UV irradiation proceeded by inserting a 5.5 W low-pressure mercury arc lamp into a micro photochemical reaction assembly with quartz well, and N₂ was smoothly flushing throughout the irradiation time at $42 \pm 1 \text{ }^\circ\text{C}$. After the irradiation was completed, 1 mL of irradiated sample was diluted with 200 mL of a NaCl-saturated aqueous solution and extracted with $6 \times 0.5 \text{ mL}$ diethyl ether. The organic layers (3 mL) were gathered, dried over Na₂SO₄ anhydrous, and analyzed by GC-MS.

GC-MS analyses of the diethyl ether extract of the irradiated samples were performed. The diethyl ether extracts were analysed by GC-MS equipped with a $15 \text{ m} \times 0.25 \text{ mm} \times 0.25 \text{ }\mu\text{m}$ TG-SQC 5% phenyl methyl polysiloxane column, with helium as carrier gas, coupled to a mass-selective detector following a specific oven program (see below). Injection volume was 0.5 μL . Identification of the reaction products was performed by comparison with the commercially available compounds by GC-MS analysis and spike experiments. Quantification of compounds was performed by multiple-point external standard calibration curves for each analyte of interest. For the reaction of cyclohexanone, 3,3-dimethyl-2-butanone, 2-hydroxycyclohexanone, and 2-cyclopenten-1-one, oven program was as follows: temperature started at 30 $^\circ\text{C}$, maintained for 10 min, increased at a rate of 25.0 $^\circ\text{C}/\text{min}$ up to 250 $^\circ\text{C}$, and held for 8 min. For the reaction of tetrahydro-4H-pyran-4-one, 4-hydroxy-4-methyl-2-pentanone, and methyl acetoacetate, oven

program was as follows: temperature started at 40 °C, maintained for 1 min, increased at a rate of 5.0 °C/min up to 110 °C, increased at a rate of 20.0 °C/min up to 250 °C, and held for 8 min.

3.3. Pulse Radiolysis

The pulse radiolysis experiments were performed with the LAE-10 linear accelerator at the Institute of Nuclear Chemistry and Technology in Warsaw, Poland, with a typical electron pulse length of 10 ns and 10 MeV of energy. A detailed description of the experimental setup has been given elsewhere along with basic details on the equipment and its data collection system [37–39].

Absorbed dose per pulse was in the order of 3.5 Gy (1 Gy = 1 J kg⁻¹). Experiments were performed with a continuous flow of sample solutions using a standard quartz cell with optical length 1 cm at room temperature (~22 °C). Solutions were purged for at least 20 min per 250 mL sample with N₂O before pulse irradiation.

The dosimetry was based on N₂O-saturated solutions of 10⁻² M KSCN, which, following radiolysis, produces (SCN)₂^{•-} radicals that have a molar absorption coefficient of 7580 M⁻¹cm⁻¹ at λ = 472 nm and are produced with a yield of G = 0.635 μmol J⁻¹ [31].

4. Conclusions

The reduction of ketones via disulfide radical anion has been obtained for the first time in an aqueous environment, following a bioinspired process connected to the known mechanism of transformation of ribonucleotides to deoxyribonucleotides. Disulfide radical anion from cysteine, (CysSSCys)^{•-}, is a very good 1e⁻ reductant, and experimental conditions were first set to obtain high-yield conversion of representative substrates. Our results can be considered as an example of bimolecular/associative reductant upconversion that has been recently reviewed [40]. Using time-resolved studies, we measured the rate constants of three cyclic aliphatic ketones to be in the range of 10⁴–10⁵ M⁻¹s⁻¹ at ~22 °C. Expansion of this methodology to other substrates and applications of disulfide radical anion in photoredox catalysis can be envisaged.

Author Contributions: Conceptualization, S.B.-V. and C.C.; methodology, S.B.-V. and K.B.; investigation, S.B.-V. and K.S.; resources, C.F. and K.B.; writing—original draft preparation, S.B.-V., K.B., and C.C.; writing—review and editing, C.F., B.M., K.B., and C.C.; supervision, K.B. and C.C. All authors have read and agreed to the published version of the manuscript.

Funding: This research received no external funding.

Institutional Review Board Statement: Not applicable.

Informed Consent Statement: Not applicable.

Data Availability Statement: The data presented in this study are available on request from the corresponding author.

Acknowledgments: Authors would like to thank Tomasz Szreder (INCT, Poland) for his continuous efforts at implementing improvements to the pulse radiolysis setup in the INCT over the last few years.

Conflicts of Interest: The authors declare no conflict of interest.

Sample Availability: Not available.

References

1. Chatgililoglu, C.; Ferreri, C.; Geacintov, N.E.; Krokidis, M.G.; Liu, Y.; Masi, A.; Shafirovich, V.; Terzidis, M.A.; Tsegay, P.S. 5',8-Cyclopurine lesions in DNA damage: Chemical, analytical, biological and diagnostic significance. *Cells* **2019**, *8*, 513. [CrossRef] [PubMed]
2. Chatgililoglu, C.; Eriksson, L.A.; Krokidis, M.G.; Masi, A.; Wang, S.-D.; Zhang, R. Oxygen dependent purine lesions in double-stranded oligodeoxynucleotides: Kinetic and computational studies highlight the mechanism for 5',8-cyclopurine formation. *J. Am. Chem. Soc.* **2020**, *142*, 5825–5833. [CrossRef]
3. Chatgililoglu, C.; Ferreri, C.; Krokidis, M.G.; Masi, A.; Terzidis, M.A. On the Relevance of Hydroxyl Radical to Purine DNA Damage. *Free Radic. Res.* **2021**. [CrossRef]

4. Chatgililoglu, C.; Ferreri, C.; Melchiorre, M.; Sansone, A.; Torreggiani, A. Lipid Geometrical Isomerism: From Chemistry to Biology and Diagnostics. *Chem. Rev.* **2014**, *114*, 255–284. [[CrossRef](#)] [[PubMed](#)]
5. Menounou, G.; Giacometti, G.; Scanferlato, R.; Dambruoso, P.; Sansone, A.; Tueros, I.; Amézaga, J.; Chatgililoglu, C.; Ferreri, C. Trans Lipid Library: Synthesis of Docosahexaenoic Acid (DHA) Monotrans Isomers and Regioisomer Identification in DHA-Containing Supplements. *Chem. Res. Toxicol.* **2018**, *31*, 191–200. [[CrossRef](#)] [[PubMed](#)]
6. Vetica, F.; Sansone, A.; Meliota, C.; Batani, G.; Roberti, M.; Chatgililoglu, C.; Ferreri, C. Free Radical-Mediated Formation of Trans-Cardiolipin isomers, Analytical Approaches for Lipidomics and Consequences for the Structural Organization of Membranes. *Biomolecules* **2020**, *10*, 1189. [[CrossRef](#)]
7. Chatgililoglu, C.; Studer, A. (Eds.) *Encyclopedia of Radical in Chemistry, Biology and Materials*; Wiley: Chichester, UK, 2012.
8. Minnihan, E.C.; Nocera, D.G.; Stubbe, J. Reversible, Long-Range Radical Transfer in E. coli Class Ia Ribonucleotide Reductase. *Acc. Chem. Res.* **2013**, *46*, 2524–2535. [[CrossRef](#)] [[PubMed](#)]
9. Greene, B.L.; Taguchi, A.T.; Stubbe, J.; Nocera, D.G. Conformationally Dynamic Radical Transfer within Ribonucleotide Reductase. *J. Am. Chem. Soc.* **2017**, *139*, 16657–16665. [[CrossRef](#)]
10. Buckel, W.; Golding, B.T. Radicals Enzymes. In *Encyclopedia of Radical in Chemistry, Biology and Materials*; Chatgililoglu, C., Studer, A., Eds.; Wiley: Chichester, UK, 2012; Volume 3, Chapter 52; pp. 1501–1546.
11. Lawrence, C.C.; Bennati, M.; Obvias, H.V.; Bar, G.; Griffin, R.G.; Stubbe, J. High-field EPR detection of a disulfide radical anion in the reduction of cytidine 5'-diphosphate by the E441Q R1 mutant of Escherichia coli ribonucleotide reductase. *Proc. Natl. Acad. Sci. USA* **1999**, *96*, 8979–8984. [[CrossRef](#)]
12. Zipse, H.; Artin, E.; Wnuk, S.; Lohman, G.J.S.; Martino, D.; Griffin, R.G.; Kacprzak, S.; Kaupp, M.; Hoffman, B.; Bennati, M.; et al. Structure of the Nucleotide Radical Formed during Reaction of CDP/TTP with the E441Q- $\alpha\beta 2$ of E. coli Ribonucleotide Reductase. *J. Am. Chem. Soc.* **2008**, *131*, 200–211. [[CrossRef](#)]
13. Barata-Vallejo, S.; Ferreri, C.; Golding, B.T.; Chatgililoglu, C. Hydrogen Sulfide: A Reagent for pH-Driven Bioinspired 1,2-Diol Mono-deoxygenation and Carbonyl Reduction in Water. *Org. Lett.* **2018**, *20*, 4290–4294. [[CrossRef](#)]
14. Ahmad, R.; Armstrong, D.A. The effect of pH and complexation on redox reactions between RS radicals and flavins. *Can. J. Chem.* **1984**, *62*, 171–177. [[CrossRef](#)]
15. Surdhar, P.S.; Armstrong, D.A. Redox-Potentials of Some Sulfur-Containing Radicals. *J. Phys. Chem.* **1986**, *90*, 5915–5917. [[CrossRef](#)]
16. Surdhar, P.S.; Armstrong, D.A. Reduction Potentials and Exchange Reaction of Thiol Radicals and Disulfide Anion Radicals. *J. Phys. Chem.* **1987**, *91*, 6532–6537. [[CrossRef](#)]
17. Armstrong, D.A. Applications of Pulse Radiolysis for the Study of Short-lived Sulphur Species. In *Sulfur-Centered Reactive Intermediates in Chemistry and Biology*; Chatgililoglu, C., Asmus, K.-D., Eds.; Plenum Press: New York, NY, USA, 1990.
18. Mezyk, S.P.; Armstrong, D.A. Disulfide anion radical equilibria: Effects of NH_3^+ , $-\text{CO}_2^-$, $-\text{NHC(O)}$ - and $-\text{CH}_3$ groups. *J. Chem. Soc. Perkin Trans.* **1999**, *2*, 1411–1419. [[CrossRef](#)]
19. Sober, H.A. (Ed.) *Handbook of Biochemistry: Selected Data for Molecular Biology*, 2nd ed.; Chemical Rubber Publishing Co.: Cleveland, OH, USA, 1970.
20. Mezyk, S.P. Determination of the Rate Constant for the Reaction of Hydroxyl and Oxide Radicals with Cysteine in Aqueous Solution. *Radiat. Res.* **1996**, *145*, 102–106. [[CrossRef](#)]
21. Mezyk, S.P. Direct rate constant measurement of radical disulphide anion formation for cysteine and cysteamine in aqueous solution. *Chem. Phys. Lett.* **1995**, *235*, 89–93. [[CrossRef](#)]
22. Knight, A.R. Photochemistry of thiols. In *The Chemistry of Thiol Group*; Patai, S., Ed.; Wiley: London, UK, 1974; Part 1; pp. 455–479.
23. Turro, N.J. *Modern Molecular Photochemistry*; University Science Books: Sausalito, CA, USA, 1991.
24. Xia, S.-H.; Liu, X.-Y.; Fang, Q.; Cui, G. Excited-State Ring-Opening Mechanism of Cyclic Ketones: A MS-CASPT2//CASSCF Study. *J. Phys. Chem. A* **2015**, *119*, 3569–3576. [[CrossRef](#)] [[PubMed](#)]
25. Shemesh, D.; Nizkorodov, S.A.; Gerber, R.B. Photochemical Reactions of Cyclohexanone: Mechanisms and Dynamics. *J. Phys. Chem. A* **2016**, *120*, 7112–7120. [[CrossRef](#)]
26. Reid, D.L.; Shustov, G.V.; Armstrong, A.A.; Rauk, A.; Schuchmann, M.N.; Akhlaq, M.S.; von Sonntag, C. H-atom abstraction from thiols by C-centered radicals. A theoretical and experimental study of reaction rates. *Phys. Chem. Chem. Phys.* **2002**, *4*, 2965–2974. [[CrossRef](#)]
27. Von Sonntag, C. *Free-Radical-Induced DNA Damage and Its Repair, A Chemical Perspective*; Springer: Berlin, Germany, 2006; p. 144.
28. Laroff, G.P.; Fessenden, R.W. Equilibrium and Kinetics of the Acid Dissociation of Several hydroxyalkyl Radicals. *J. Phys. Chem.* **1973**, *77*, 1283–1288. [[CrossRef](#)]
29. Xu, L.; Jin, J.; Lai, M.; Daublain, P.; Newcomb, M. Compatible Injection and Detection Systems for Studying the Kinetics of Excess Electron Transfer. *Org. Lett.* **2007**, *9*, 1837–1840. [[CrossRef](#)] [[PubMed](#)]
30. Yayla, H.G.; Knowles, R.R. Proton-Coupled Electron Transfer in Organic Synthesis: Novel Homolytic Bond Activation and Catalytic Asymmetric Reactions with Free Radicals. *Synlett* **2014**, *25*, 2819–2826. [[CrossRef](#)]
31. Janata, E.; Schuler, R.H. Rate constant for scavenging e^-_{aq} in N_2O -saturated solutions. *J. Phys. Chem.* **1982**, *86*, 2078–2084. [[CrossRef](#)]
32. Péter, A.; Agasti, S.; Knowles, O.; Pye, E.; Procter, D.J. Recent advances in the chemistry of ketyl radicals. *Chem. Soc. Rev.* **2021**, *50*, 5349–5365. [[CrossRef](#)] [[PubMed](#)]
33. Huffman, J.W. Metal-Ammonia Reductions of Cyclic Aliphatic Ketones. *Acc. Chem. Res.* **1983**, *16*, 399–405. [[CrossRef](#)]

34. Buxton, G.V.; Greenstock, C.L.; Helman, W.P.; Ross, A.B. Critical review of rate constants for reactions of hydrated electrons, hydrogen atoms and hydroxyl radicals (OH/O⁻) in aqueous solution. *J. Phys. Chem. Ref. Data* **1988**, *17*, 513–886. [[CrossRef](#)]
35. Hoffman, M.Z.; Hayon, E. One-Electron Reduction of the Disulfide Linkage in Aqueous Solution. Formation, Protonation, and Decay Kinetics of the RSSR- Radical. *J. Am. Chem. Soc.* **1972**, *94*, 795–7957. [[CrossRef](#)]
36. Schaefer, T.; Herrmann, H. Competition kinetics of OH radical reactions with oxygenated organic compounds in aqueous solution: Rate constants and internal optical absorption effects. *Phys. Chem. Chem. Phys.* **2018**, *20*, 10939–10948. [[CrossRef](#)]
37. Bobrowski, K. Free radicals in chemistry, biology, and medicine: Contribution of radiation chemistry. *Nukleonika* **2005**, *50* (Suppl. 3), S67–S76.
38. Mirkowski, J.; Wisniowski, P.; Bobrowski, K. *INCT Annual Report 2000*; INCT: Warsaw, Poland, 2001.
39. Pedzinski, T.; Grzyb, K.; Skotnicki, K.; Filipiak, P.; Bobrowski, K.; Chatgililoglu, C.; Marciniak, B. Radiation- and Photo-Induced Oxidation Pathways of Methionine in Model Peptide Backbone under Anoxic Conditions. *Int. J. Mol. Sci.* **2021**, *22*, 4773. [[CrossRef](#)] [[PubMed](#)]
40. Syroeshkin, M.A.; Kuriakose, F.; Saverina, E.A.; Timofeeva, V.A.; Egorov, M.P.; Alabugin, I.V. Upconversion of Reductants. *Angew. Chem. Int. Ed.* **2019**, *58*, 5532–5550. [[CrossRef](#)] [[PubMed](#)]